Synthesis of High Specific Surface Lithium ion Sieve Templated by Bacterial Cellulose for Selective Adsorption of Li+

Xudong Zheng (Zhengks@outlook.com)
Changzhou University https://orcid.org/0000-0003-2688-4855
Ang Li
Changzhou University
Dandan Wang
Changzhou University
Da Xia
Changzhou University
Yuzhe Zhang
Changzhou University
Zhongyu Li
Changzhou University

Research Article

Keywords: Lithium ion sieve, Bacterial cellulose, Hydrothermal method, Titanium, Selective adsorption

Posted Date: June 21st, 2021

DOI: https://doi.org/10.21203/rs.3.rs-580568/v1

ipSynthesis of high specific surface lithium ion sieve templated by bacterial cellulose for selective adsorption of Li^+

Xudong Zheng*, Ang Li, Dandan Wang, Da Xia, Yuzhe Zhang, Zhongyu Li*

*Correspondence to: X. Zheng (E-mail: zhengks@outlook.com); Z. Li (E-mail: zhongyuli@mail.tsinghua.edu.cn);

Graphical Abstract

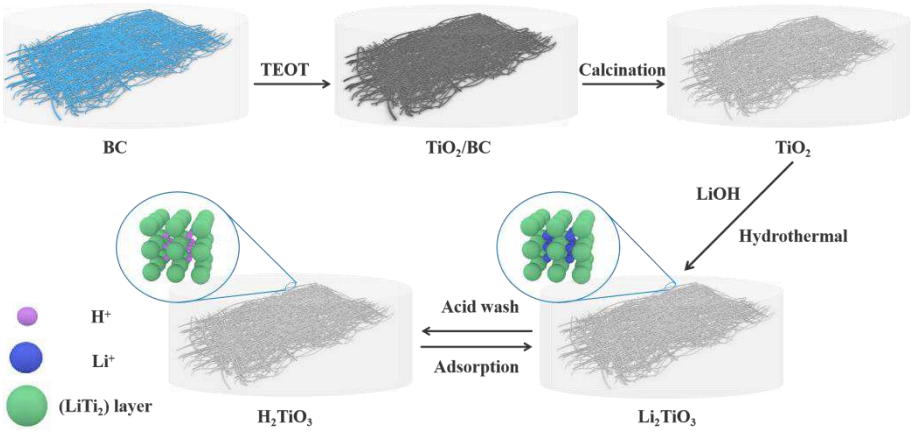

Lithium ion sieve templated by bacterial cellulose for selective adsorption of Li^+

Abstract

In recent years, the lithium market has ushered in a golden period of development. With the development of batteries, ceramics, glass, lubricants, refrigerants, the nuclear industry and the optoelectronics industry, the demand for lithium has grown rapidly, and continuous mining has led to scarcity of land resources. On the other hand, due to the rich lithium resources in sea water and salt lake brines. How to selectively adsorb and separate lithium ions from seawater and salt lake brine has attracted more and more scholars' attention and research. Lithium ion sieve stands out because of its excellent performance of specific adsorption and separation of lithium ions. This article reports the preparation of mesoporous TiO_2 and LiOH hydrothermal reaction using bacterial cellulose as a biological template. After calcination at 600°C, spinel lithium titanium oxide Li_2TiO_3 is formed. H_2TiO_3 was obtained by eluting the precursor with HCl eluent. FT-IR, SEM and XRD were used to characterize Li_2TiO_3 and H_2TiO_3. The adsorption performance of H_2TiO_3 was

studied through adsorption pH, adsorption kinetics, adsorption isotherms, competitive adsorption and so on. The results show that H_2TiO_3 is a single layer chemical adsorption process, which has a good adsorption effect on lithium ions at pH 11.0, with the maximum adsorption capacity can reach 35.45 $mg \cdot g^{-1}$. The lithium ion sieve has selective adsorption to Li^+, and its distribution coefficient is 2242.548 mL g^{-1}. It may be predicted that the lithium-ion sieve prepared by biological template has a broad application prospect.

Keywords: Lithium ion sieve; Bacterial cellulose; Hydrothermal method; Titanium; Selective adsorption

1. Introduction

Lithium is the rarest element among alkali metals(Zeng et al. 2018). It is the lightest silver-white metal with strong chemical activity, can synthesize inorganic and organic compounds of lithium with various elements. Lithium and a variety of metals constitute light alloys, wear-resistant alloys, etc. Al-Li and Mg-Li alloys will become new structural materials for the next generation of aerospace industry. Lithium resources in China are mainly distributed in Qinghai-Tibet Plateau, Xinjiang, Inner Mongolia, Sichuan and Jiangxi, accounting for 25.6 % of the world's lithium reserves, ranking second in the world(DING et al. 2018). Among them, salt lake brine lithium resources are the main form of lithium resources in China, accounting for about 85 % of the total proved lithium reserves in China(Liu et al. 2021). Therefore, it is very important to study how to transform lithium extraction technology and extract lithium efficiently from Salt Lake brine(Argurio et al. 2019). At present, there are many known methods for adsorption and separation of lithium Li^+ from salt lake brine. For example, precipitation method(Song et al. 2017), electrochemical method(Romero et al. 2018), solvent extraction method(Gza et al. 2020; Zhao et al. 2017), ion exchange method(Grágeda et al. 2018; Michel et al. 2018) and so on. Among them, ion-exchange method stands out from many lithium extraction methods because of its simple process, high recovery rate and economic and green advantages(Ma et al. 2018). Compared with some natural inorganic minerals and carbon materials(Wen et al. 2017), there is a lack of adsorption selectivity(Lihua et al. 2018) for Li^+. Lithium

ion sieve has the characteristics of selective adsorption of Li^+ because it is first inserted into the precursor by Li^+ and then eluted by eluent(Peng et al. 2019). As the main representative of lithium ion sieves, spinel manganese oxide ion sieves have high specific adsorption for Li^+ after acid elution of precursors. For example, Gao A, Sun Z and others synthesized representative adsorbent $Li_{1.6}Mn_{1.6}O_4$ for lithium ion sieves(Gao et al. 2018). Its maximum adsorption capacity can reach 44 $mg \cdot g^{-1}$. Similarly, Yang, Shan Shan, Zhou, Ma Li, Ma Li et al. Through LiOH, $Mn(CH_3COO)_2$, H_2O_2 and ethanol, using sol gel method, hydrothermal method and low-temperature solid-phase method combined with manganese oxide lithium ion sieve made a series of research(Yang et al. 2016). Keiko Sasaki and Qianqian Yu and their colleagues synthesized a lithium ion sieve with microtubule morphology using manganese-oxidizing fungus as biological template by calcination solid-phase bonding. The effect of adsorption capacity at different calcination temperatures was studied. The structural and morphological characterization and adsorption experiments show that the weight fraction of spinel lithium manganese oxide ion sieve also changes with different calcination temperatures, and it will affect its crystallinity, so the choice of calcination temperature directly affects the adsorption capacity of lithium ion sieve(Sasaki and Yu 2015). Song et al. Spinel structure $Li_{1+x}Mn_{2-x}O_4$ materials for lithium ion-sieve precursor were synthesized by high temperature solid state method. The results showed that the $Li_{1.3}Mn_{1.7}O_4$ material had the largest adsorption capacity and it reached up to 24.06 $mg \cdot g^{-1}$ when the pH value was 12 and the adsorption time was 10 h(Img et al. 2021). However, the current Li-Mn-O ion sieve have the same shortcomings in the process of acid pickling: the appearance of Mn^{2+} in the process of elution causes partial dissolution of the ion sieves, which reduces the repeatability of the lithium ion sieves. On the other hand, the appearance of titanium-based lithium ion sieves compensated for the dissolution of Ti during acid pickling. For example, Shulei Wang, Ping Li and others synthesized β-Li_2TiO_3 by hydrothermal method of TiO_2 and $LiOH \cdot H_2O$(Zhang et al. 2019). Compared with manganese ion sieves, the dissolution rate of Ti is also reduced while Li^+ is highly selectively adsorbed by manganese ion sieves. Cheng-Long Yua,

Kazumichi Yanagisawa et al, synthesized pure Li_2TiO_3 nanoparticles by hydrothermal reaction of anatase TiO_2 and $LiOH·H_2O$, and studied the formation of Li_2TiO_3, the diffusion and insertion mechanism of lithium ions(Garay-Rodríguez et al. 2019). Ramesh et al. Anatase type TiO_2 and Li_2CO_3 were mixed, ground and heated in an alumina crucible at 700 °C in air to obtain the lithium ion sieve precursor (Li_2CO_3). The measured adsorption capacity of the adsorbent is 32.6 $mg·g^{-1}$(Garcia et al. 2018b). Unfortunately, most of the known lithium ion sieves are powdered, which is not conducive to the mass production of ion sieves in practical applications. Therefore, the preparation of mesoporous nanomaterials to synthesize lithium ion sieve is of special significance(Elik et al. 2018). Cellulose is a polysaccharide with a wide coverage and the largest content in nature(Li et al. 2019). Rich content and low price make it naturally attract the attention of scientific researchers in recent years. However, natural cellulose has some impurities such as lignin and hemicellulose, especially the coarse fiber diameter of natural cellulose, which affects the performance of cellulose(Tomer and Malik 2019). With the in-depth of bacterial cellulose (BC) synthesized by microorganisms under different conditions, the chemical structure of BC is the same as that of plant cellulose(Aimar et al. 2019). The difference is that BC has the advantages of higher purity and finer fiber diameter than plant cellulose. Due to the formation of ultrafine network structure of bacterial cellulose and the "nano-effect", bacterial cellulose has the characteristics of high water absorption and water retention, high permeability to liquids and gases, high wet strength, and in-situ processing and moulding, especially in wet state. High purity and excellent performance can be widely used in many fields.

As far as we know, there is no report about the preparation of Li_2TiO_3 by hydrothermal reaction using bacterial cellulose as template. Thus, in this research, We first proposed using BC as a template to form titanium dioxide mesoporous membrane on the substrate. Then, the precursor of Li_2TiO_3 was preliminarily obtained by hydrothermal method with LiOH(Garcia et al. 2018a). The morphology of the precursor was stabilized by calcination at high temperature and the lithium ion sieve with mesoporous shape was obtained by acid elution. Finally, we also proved the

excellent adsorption effect of this lithium ion sieve using bacterial cellulose as template in the adsorption experiment, and expected its application prospects.

2. Experimental

2.1 Synthesis of the Li_2TiO_3

Bacterial cellulose (BC) hydrogel, titanium ethoxide (TEOT), lithium hydroxide (LiOH). Deionized water was used in all experiments. Hydrochloric acid (HCl) and other drugs used are analytically pure, without the need for further processing and purification. Bacterial cellulose (BC) hydrogel was placed in deionized water for 15 min to achieve swelling effect. After freezing with liquid nitrogen and freeze-drying, the bacterial cellulose (BC) aerogel with a network structure was obtained. The bacterial cellulose (BC) aerogel was immersed in titanium ethoxide (TEOT) solution for 2 h. Then, after alternately rinsing with ethanol and ultrapure water for 4 to 5 times, it was placed in ultrapure water and mechanically stirred for 2 hours, and the product was repeatedly washed with deionized water. Finally, the bacterial cellulose film material TiO_2/BC wrapped in TiO_2 was obtained after drying in the oven(Zhu et al. 2020). TiO_2 with a weight of 0.826 g was obtained by calcining at 600 ℃ for 6 h at 4 °C/ min in a tubular furnace. The TiO_2 was dissolved in 10.45 ml of H_2O with 0.5 g of LiOH. The Li: Ti molar ratio of 2:1, unstable spinel Li_2TiO_3 is obtained after hydrothermal reaction at 180 °C for 18 h. The stable spinel Li_2TiO_3 was obtained after being calcined at 4 °C/ min at 600 °C for 6 h in a tube furnace.

2.2 Synthesis of the H_2TiO_3

Li_2TiO_3 was eluted in the 0.1 mol/L of HCl at 65 °C for 12 h, and then the eluate was changed again to ensure the elution. Finally, the eluted product was washed and filtered with ultra-pure water and dried in an oven at 70 °C. The final product was spinel titanium oxide ion screen. The titanium based lithium ion sieves H_2TiO_3 with high adsorption and specific adsorption for Li^+ were obtained.

3. Results and discussion

Characterizations of Li_2TiO_3 and H_2TiO_3

In order to analyze functional groups of TiO_2, Li_2TiO_3 and H_2TiO_3, FT-IR analysis was performed and presented in Figure 1. Broad peaks at 3448 and 2925 cm^{-1}

were observed for three materials' FT-IR spectra, which can be interpreted as O-H and C-H stretching vibrations, respectively. Among them, OH peak was observed. This peak was due to the isolated O-H bond not participating in the interaction with other hydroxyl groups. In addition, compared with the FT-IR spectra of TiO_2, the new peaks at 1438 and 1508 cm^{-1} appeared after lithium insertion, which belonged to the characteristics vibration of Li-O-Ti band. It indicates that the precursor (Li_2TiO_3) was formed. In the case of Li_2TiO_3, the disappearance of peaks at 1438 and 1508 cm^{-1} show successful elution of lithium ions, and the preparation of lithium ion sieve (H_2TiO_3) was completed. As can be seen in the SEM diagram in Figure 2(a), the titania films formed with bacterial cellulose as template feature pronounced high pore volume network structure. After the hydrothermal calcination with LiOH, the films become denser with crystals grow and aggregate, resulting in the formation of spinel Li_2TiO_3 (Figure 2b). The nitrogen sorption data of H_2TiO_3 showed a BET surface area of 27.4006 m^2/g. Based on the adsorption desorption isotherm of nitrogen (Figure 3) shows that the pore structure in the material is consistent with the results of SEM. It can further be inferred that bacterial cellulose as template is effective.

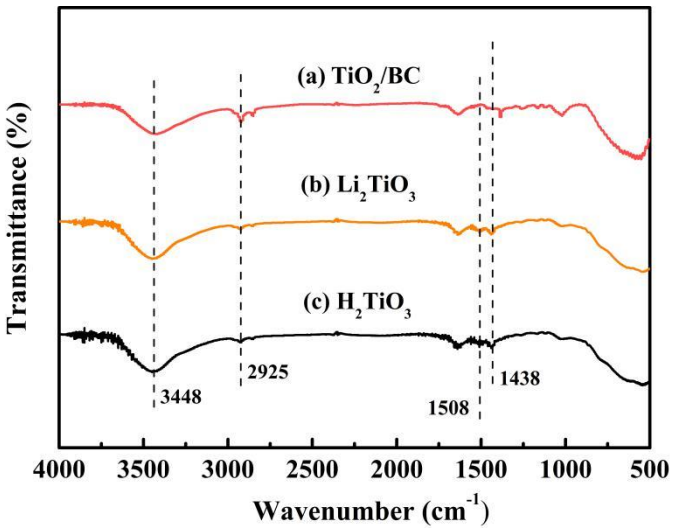

Fig. 1 (a) FT-IR spectra of TiO_2/BC; (b) Li_2TiO_3; (c) H_2TiO_3

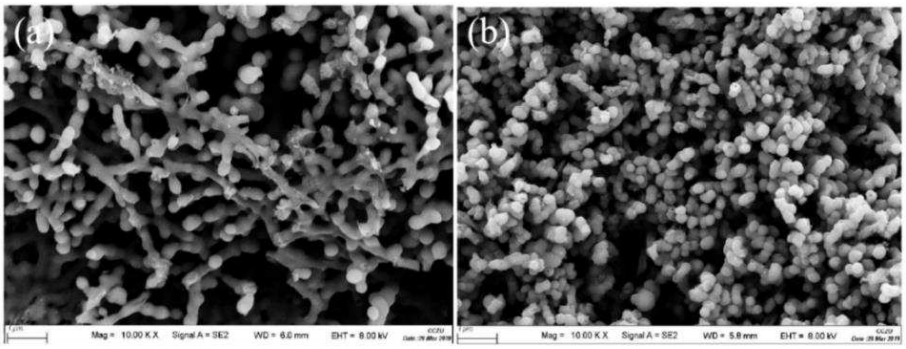

Fig. 2 (a) SEM image of TiO_2/BC; (b) SEM images of Li_2TiO_3.

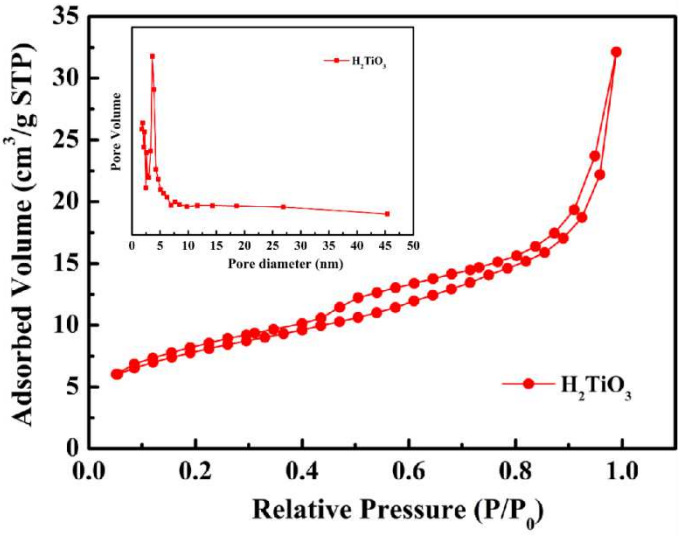

Fig. 3 Nitrogen adsorption-desorption isotherm of H_2TiO_3. Inset showing Inset showing pore size distributions.

As shown in Figure. 4, XRD pattern of the Li_2TiO_3 before calcination, Li_2TiO_3 after calcination and H_2TiO_3 were collected at the 2θ angle from 10 to 70°. In the XRD pattern of the Li_2TiO_3, a new diffraction peak at (002) appeared after calcination, which belonged to the growth of (002) diffraction peak needs higher calcination temperature(Gebreslase and Technology 2018). The occurrence of diffraction peaks of (002), (-133), (-206) and (062) can be seen in the Figure 4(b), indicating that Li^+ is orderedly inserted into TiO_2,which were matched well with the pure monoclinic crystal of Li_2TiO_3(Peng et al. 2019). After eluting, the position of the diffraction peaks can be observed to be about the same, and the diffraction peak of (-133) and (-206) almost disappears, which proves on exchange occurs in Li^+/H^+ and the formation of H_2TiO_3 structure.

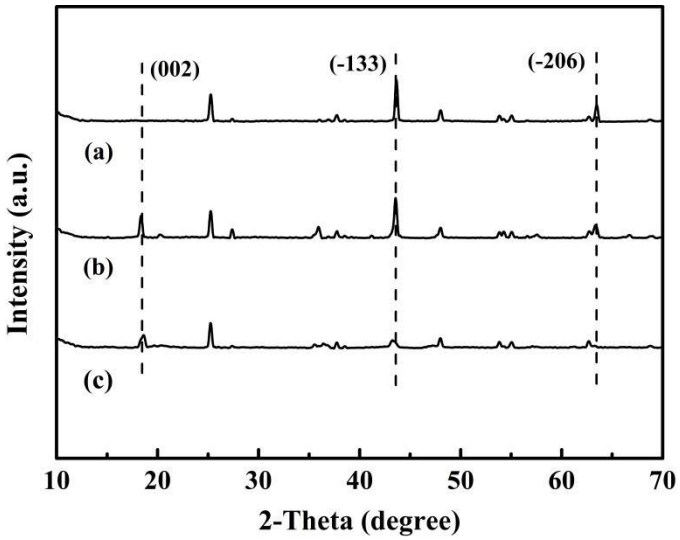

Fig. 4 (a) XRD patterns of Li_2TiO_3 before calcination; (b) Li_2TiO_3 after calcination; (c) H_2TiO_3

4. Adsorption performance of H_2TiO_3

4.1 Effect of pH

Here we briefly explore the relationships between Li^+ and its adsorption mechanism, in which the pH value dominates the study. The pH value is particularly critical for the adsorption capacity of H_2TiO_3. As shown in Fig. 5a, with the pH value increases, the adsorption amount of Li^+ also increases gradually(Sw et al.). It can be seen that the adsorption of Li^+ is favorable under alkaline condition. In order to avoid adding more NaOH to adjust the higher pH concentration, thus increasing the effect of cations in the solutions and considering that the excessively high pH value is not conducive to mass production in industrial applications. Therefore, the recovery of Li^+ in this experiment was mainly carried out at pH 11. Fig. 5b shows the zeta potential test of lithium ion sieve. with the pH increases, the value of the electrostatic negative charge value on the material also gradually increases. It keeps coincident with the pH tests results.

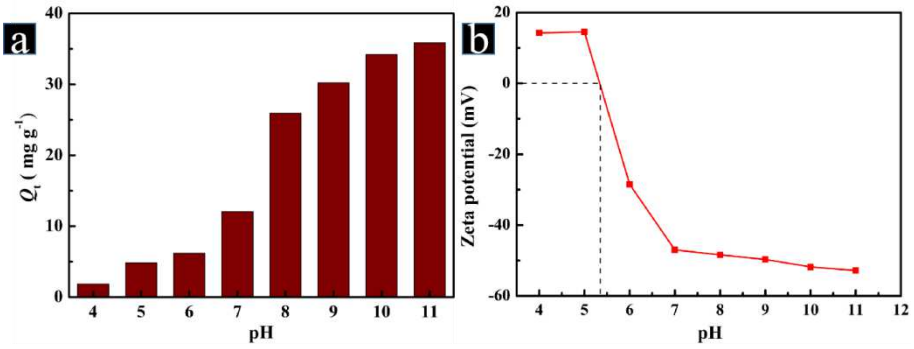

Fig. 5 (a) Effect of pH on adsorption capacities (b) Zeta potential measurement of H_2TiO_3

4.2. Adsorption kinetics

Through the adsorption kinetics experiment, the connection between the adsorption amount (Q_t) and the adsorption time (t) was analyzed. We can see in Figure 6, the adsorption curve of the ion sieve adsorbent increased rapidly from the begining, reaching about 80% of the maximum adsorption capacity at 200 min, then the adsorption curve increases slightly and eventually gradually tends to adsorption equilibrium at about 6 h. The adsorption process of ionic sieve H_2TiO_3 in LiCl solution was fitted by pseudo-first-order kinetic model (PFOKM), pseudo-second-order kinetic model (PSOKM) to explore the adsorption rate constant and mechanism. The fittting equation of the PFOKM and PSOKM as follows:

$$Q_t = Q_e - Q_e e^{-k_1 t} \quad (1)$$

$$Q_t = \frac{k_2 Q_e^2 t}{1 + k_2 Q_e t} \quad (2)$$

Where, Q_t (mg·g^{-1}) corresponds to the amount of Li^+ adsorbed at time t(min) and Q_e (mg·g^{-1}) corresponds to the amount of adsorption at equilibrium. k_1 (min^{-1}) and k_2 (g·mg^{-1}·min^{-1}) are the rate constants of the PFOKM and PSOKM, respectively. In addition, the h (mg·g^{-1}·min^{-1}) and $t_{1/2}$ (min) of the PSOKM are listed in the following formulas (3) and (4):

$$h = k_2 Q_e^2 \quad (3)$$

$$t_{1/2} = \frac{1}{k_2 Q_e} \quad (4)$$

The kinetic curve of adsorption was fitted by PFOKM and PSOKM. The fitting curve and corresponding parameters are presented in Figure 6 and Table 1, respectively. Obviously, the correlation coefficient of R^2 fitted by PSOKM is larger

than the correlation coefficient of R^2 fitted by PFOKM, which better matches the experimental data.

At the same time, the equilibrium adsorption amount calculated based on the PFOKM and the PSOKM. Compared with the actual values, the results of the pseudo-secondary dynamics model are closer to reality. Therefore, we believe that PSOKM is more in line with the adsorption of ion sieve H_2TiO_3 in LiCl solution. This further illustrates that the adsorption process of Li^+ by H_2TiO_3 is mainly completed under the chemical action.

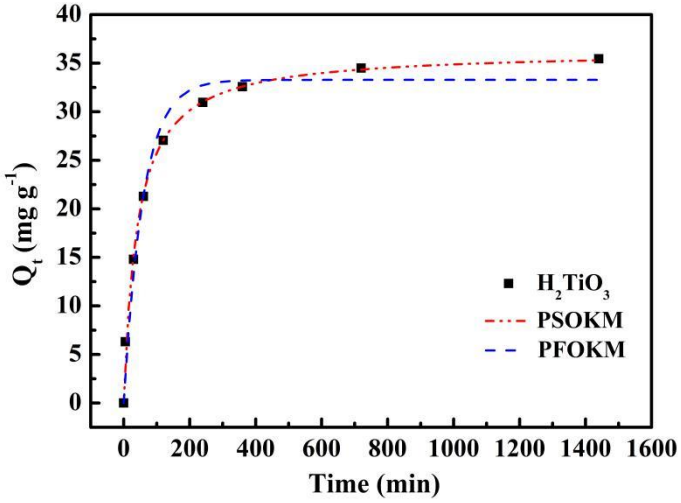

Fig.6 Kinetic data and modeling for the adsorption of Li^+: Fitting curves of PFOKM and PSOKM

Table 1. Kinetic parameters for the PFOKM and PSOKM

Sorbents	$Q_{e,exp}$ $(mg \cdot g^{-1})$	*PFOKM*			*PSOKM*		
		$Q_{e,c}$ $(mg \cdot g^{-1})$	k_1 (min^{-1})	R^2	$Q_{e,c}$ $(mg \cdot g^{-1})$	$k_2 \times 10^{-2}$ $(g \cdot mg^{-1} \cdot min^{-1})$	R^2
H_2TiO_3	35.45	33.28	0.0172	0.975	36.29	0.068	0.991

4.3. Adsorption isotherms

By statically testing equilibrium adsorption data and adsorption curves in LiCl solutions (100-2000 $mg \cdot L^{-1}$), so as to explore the equilibrium concentration and adsorption amount of the adsorbent in different concentrations of lithium-containing solutions. Among them, from the curve fitted by Langmuir and Freundlich equation (Figure 7), the adsorption effect will become higher with the increase of Li^+ concentration. The saturation adsorption capacity of H_2TiO_3 is 35.45 $mg \cdot g^{-1}$. The related isothermal constants are listed Table 2. It is not difficult to see that the

correlation parameters of the Langmuir and Freundlich adsorption isotherm models are R^2=0.996 and R^2=0.978, respectively. In comparison, the Langmuir isotherm adsorption model can better match the experimental data, which also corresponds to the single layer adsorption. This indicates that fitting experimental data with Langmuir equation is closer to actual data. Hence, the lithium ion sieve is known as an adsorbent with excellent performance in extracting Li^+. Experimental data fit via Langmuir and Freundlich models, which were calculated by Eqs. (5) and (6):

$$Q_e = \frac{K_L Q_m C_e}{1 + K_L C_e} \tag{5}$$

$$Q_e = K_F C_e^{1/n} \tag{6}$$

In the formula, Q_m (mg·g^{-1}) is expressed as the maximum amount of H_2TiO_3 to Li^+. K_L (L g^{-1}) corresponds to the Langmuir isotherm constant. K_F (mg·g^{-1}) corresponds to Freundlich isotherm direction constant, 1/n corresponds to the effect of concentration on the amount of adsorption, R_L is used as a separation factor to identify the merits of H_2TiO_3, which the calculation formula of R_L is listed in formula (7):

$$R_L = \frac{1}{1 + C_m K_L} \tag{7}$$

In this formula, C_m is explained as the maximum initial concentration of Li^+.

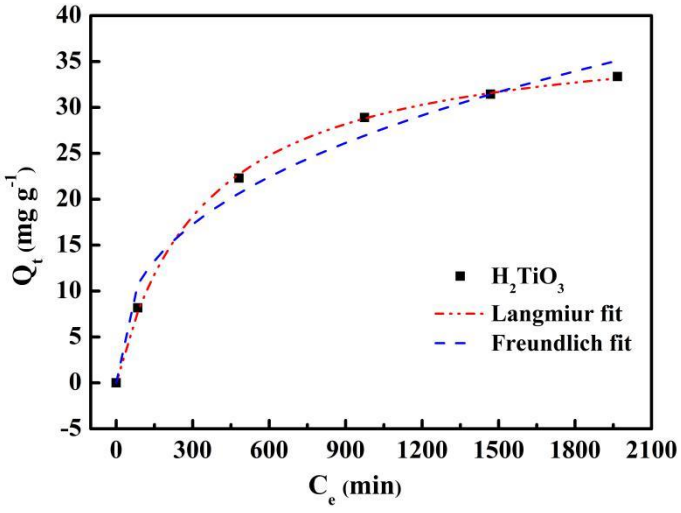

Fig.7 Isotherm model fitting of on H_2TiO_3 adsorbing Li^+.

Table 2. Adsorption equilibrium constants of Langmuir and Freundlich models

Sorbents	*Langmuir isotherm model*			*Freundlich isotherm model*		
	Q_m (mg·g^{-1})	K_L (L·mg^{-1})	R^2	K_F (mg·g^{-1})	1/n	R^2
H_2TiO_3	38.96	0.003	0.998	2.01	0.38	0.948

4.4. Effect of temperature

Further, considering the influence of thermal motion characteristics on the adsorption efficiency. Therefore, we explored the effect of H_2TiO_3 on Li^+ adsorption at different temperatures (298.15 K, 308.15 K, and 318.15 K) through thermodynamic experiments. ΔG° is calculated from the Gibbs free energy formula, and the change of Q_e with temperature was studied (Fig. 8 (a)). ΔH° and ΔS° are calculated by the lnK° equation, and the change of van't Hoff plot of lnK° to 1/T was studied (Fig. 8 (b))(Zhang et al.). The results of the thermodynamic parameters of the ion sieve are shown in Table 3. It can be observed that at a temperature of 298.15-318.15K, the value of ΔG° is maintained at -3.85 to -4.73 kJ·mol^{-1}, and is always negative. It indicates that as the temperature increases, the adsorption capacity will gradually become higher. That is to say, the adsorption of Li^+ is a spontaneous process. At the same time, ΔH° is always positive, which can be explained as an endothermic adsorption process, indicating that the Li^+ adsorption effect will increase with increasing temperature. Hence, we believe that the adsorption of Li^+ on the ion sieve is a spontaneous endothermic process.

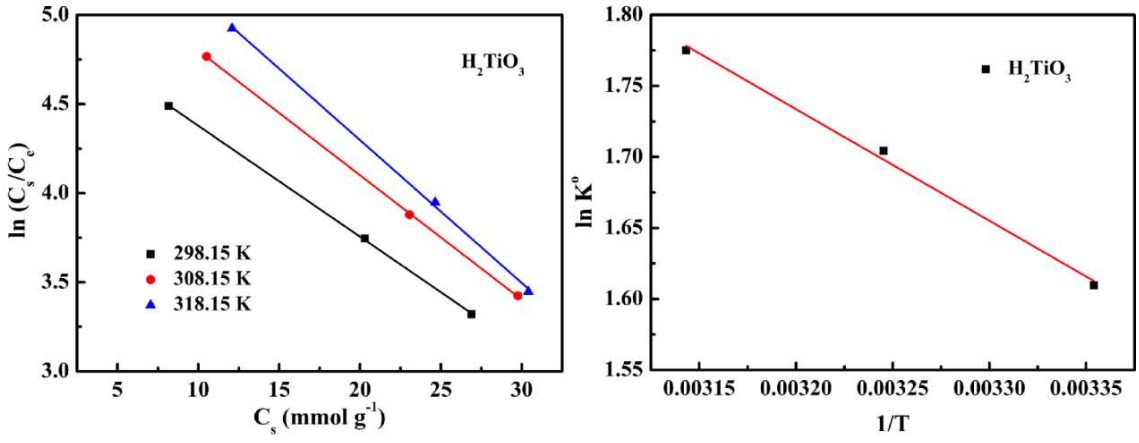

Fig. 8 Thermodynamic properties of Li^+ on H_2TiO_3 at 298.15, 308.15, and 318.15 K

Table 3. Thermodynamic parameters for Li^+ adsorption

Sorbents	ΔH^o *(kJ mol^{-1})*	ΔS^o *(J mol^{-1})*	*T (K)*	K^o	ΔG^o *(kJ mol^{-1})*	R^2
H_2TiO_3	6.54	35.31	298.15	5.00	-3.99	0.992
			308.15	5.50	-4.37	
			318.15	5.90	-4.70	

4.5. Selective and reusability tests

Through selective experiments to determine whether H_2TiO_3 has a specific adsorption selectivity for Li^+, we simulated salt lake brine for competitive adsorption experiment, and tested the adsorption performance of H_2TiO_3 to Na^+, Mg^{2+}, K^+, Ca^{2+}, Li^+. K_d (mL·g^{-1}) is the partition coefficient and k as the selectivity coefficient were used as indicators to evaluate the selectivity of H_2TiO_3. According to the magnitude of the comparison K_d value, the adsorption selection performance of H_2TiO_3 for Li^+ can be judged. From the experimental results, we can clearly observe that when the adsorption reaches equilibrium, the adsorption effect and partition coefficient (K_d) of Li^+ by H_2TiO_3 are several times that of other metal ions. Based on this, it can be determined that the lithium ion sieve H_2TiO_3 specifically adsorbs Li^+. The selectivity of ion sieve for Li^+ K^+ Ca^{2+} Na^+ Mg^{2+} was assessed by distribution coefficient (K_d, mL g^{-1}), which is listed in formula (8):

$$k_d = \frac{C_o - C_f}{C_f} \times \frac{V}{m} \tag{8}$$

In this formula, C_0 is interpreted as the initial concentration of five ionic solutions, and C_f represents the final concentration of each ionic solution.

The industrial feasibility of lithium ion sieve was verified by adsorption cycle experiment, so that the production cost was minimized. After each adsorption, the eluent (0.1M HCl) desorbs the adsorbent. Such a process is called a cycle. The experimental results are shown in Fig. 11. After 5 cycles, the capacity of the adsorbent remained above 82% of the initial value. All these results confirm that H_2TiO_3 has a good cycle adsorption potential for Li^+.

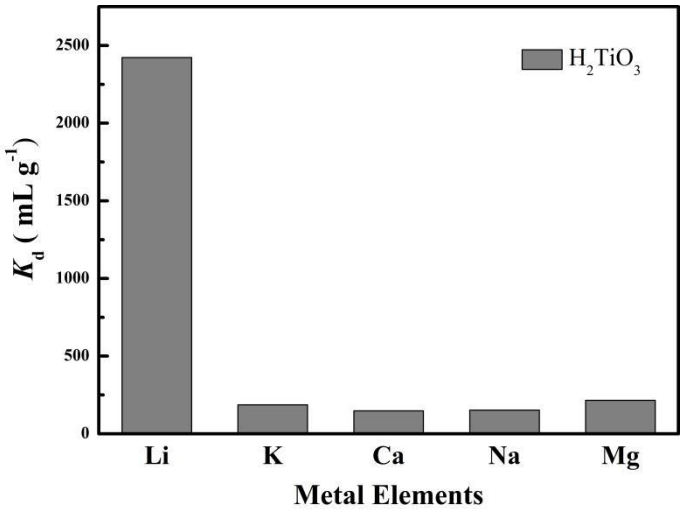

Fig.9 K_d values of H_2TiO_3 for a mixture of Na^+, Mg^{2+}, K^+, Ca^{2+}, Li^+

Table 4. K_d and k values of H_2TiO_3

Cation	H_2TiO_3		
	C_f (mg·L^{-1})	K_d (mL·g^{-1})	k
Li^+	14.609	2422.548	
K^+	48.059	40.388	0.017
Ca^{2+}	45.961	87.879	2.176
Na^+	47.634	49.670	0.565
Mg^{2+}	44.087	134.121	2.700

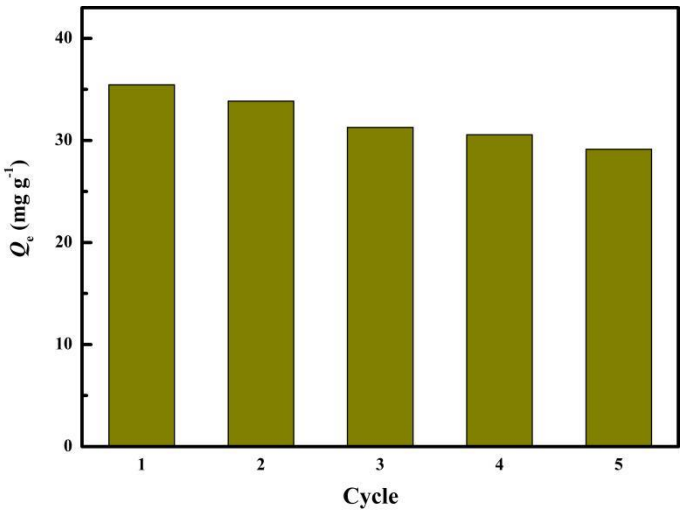

Fig.10 Regeneration of H_2TiO_3 5 cycles.

4. Conclusion

In this study, a lithium ion sieve with bacterial cellulose as a template was successfully prepared and used for the specific adsorption and separation of Li^+ from seawater and salt lake brine. And it shows excellent periodicity and stability in

adsorption, elution and circulation experiments. At the same time, using bacterial cellulose as a biological template, the preparation of mesoporous titanium-based lithium ion sieve was realized. Compared with the previous methods of assembling lithium-ion sieve, the ion sieve prepared by using cellulose as biological template not only has a slightly higher adsorption capacity, but also has the mesoporous structure provided by bacterial cellulose, which provides more possibilities for future research. Therefore, we believe that the spinel-type titanium dioxide ion sieve prepared by this method has broad application prospects and is expected to be widely used.

Acknowledgements

This work was funded through National Natural Science Foundation of China [No.21808018, 21876015，21878026]; Jiangsu Provincial Science and Technology Department Industry Foresight Plan [No. FZ20180422]; Natural science research project of colleges and universities in Jiangsu Province [No.18KJB610002] and Applied Basic Research in Changzhou [No. CJ20180055]. The authors also expressed their gratitude to other testers in this study.

Declarations

Conflict of interest

The authors declare that they have no conflict of interest.

Ethical approval

The article does not contain any experiments with human participants or animals performed by any of the authors.

Informed consent

Informed consent was obtained from all individual participants included in the st udy

References

Aimar A, Palermo A, Innocenti BJJoHE (2019) The Role of 3D Printing in Medical Applications: A State of the Art 2019:1-10

Argurio P, Tagarelli A, Molinari R (2019) A Study on Neodymium Recovery from Aqueous Solutions for Designing a New Generation of Sandwich Liquid Membrane

DING et al. (2018) Genesis of the Weiquan Ag-Polymetallic Deposit in East Tianshan, China:Evidence from Zircon U-Pb Geochronology and C-H-O-S-Pb Isotope Systematics v.92:222-244

Elik A, Topu G, Isik T, Baba A, Horzum N, De mir MM Investigation of Lithium Sorption Efficiency Using SWCNT Functionalized Electrospun Fiber Mats from the Hypersaline Geothermal Brine. In: Materials Science Forum, 2018.

Gao A, Sun Z, Li S, Hou X, Li H, Wu Q, Xi XJDT (2018) The mechanism of manganese dissolution on Li1.6Mn1.6O4 ion sieves with HCl 47:3864-3871

Garay-Rodríguez L, Murcia-López S, Andreu T, Moctezuma E, Torres-Martínez L, Morante JRJC (2019) Photocatalytic Hydrogen Evolution Using Bi-Metallic (Ni/Pt) Na2Ti3O7 Whiskers: Effect of the Deposition Order 9

Garcia, Eric, M., Taroco, Hosane, Recycling AJ (2018a) Water Electrolysis Anode Based on 430 Stainless Steel Coated with Cobalt Recycled from Li-Ion Batteries 3:42-42

Garcia, Eric M, Taroco, Hosane A, Teixeira, Rodrigo GJR (2018b) Fast Electrochemical Method for Organic Dye Decolorization Using Recycled Li-Ion Batteries

Gebreslase GAJJoMS, Technology (2018) Review on Membranes for the Filtration of Aqueous Based Solution: Oil in Water Emulsion 08

Grágeda M, González A, Grágeda M, Ushak SJIJoER (2018) Purification of brines by chemical precipitation and ion-exchange processes for obtaining battery-grade lithium compounds

Gza B, Dt A, Mb AJAG (2020) Solvent extraction of lithium from simulated shale gas produced water with a bifunctional ionic liquid - ScienceDirect 123

Img A, Avv A, Vmv B (2021) Thermal dependency of Li + -ion conductivity in Li 2 O-Fe 2 O 3 -Al 2 O 3 ceramics

Li M, Miao Y, Zhai X, Yin Y, Liu ZJM, design (2019) Preparation of and research on bioinspired graphene oxide/nanocellulose/polydopamine ternary artificial nacre 181:107961

Lihua et al. (2018) New Insights into the Application of Lithium-Ion Battery Materials: Selective Extraction of Lithium from Brines via a Rocking-Chair Lithium-Ion Battery System

Liu L, Feng X, Rahe C, Li W, Ouyang MJJoEC (2021) Internal short circuit evaluation and corresponding failure mode analysis for lithium-ion batteries

Ma L, Xi X, Wang K, Zhao LJRoCI (2018) Adsorption of Li by a lithium ion-sieve using a buffer system and application for the recovery of Li from a spent lithium-ion battery:1-19

Michel C, Barré Y, Guiza MB, Dieuleveult CD, Windt LD, Grandjean AJCEJ (2018) Breakthrough studies of the adsorption of Cs from freshwater using a mesoporous silica material containing ferrocyanide 339:288-295

Peng C, Liu F, Wang Z, Wilson BP, Lundstrom MJJoPS (2019) Selective extraction of lithium (Li) and preparation of battery grade lithium carbonate (Li 2 CO 3) from spent Li-ion batteries in nitrate system 415:179-188

Romero VCE, Tagliazucchi M, Flexer V, Ca Lvo EJJJoTES (2018) Sustainable Electrochemical Extraction of Lithium from Natural Brine for Renewable Energy Storage 165:A2294-A2302

Sasaki K, Yu Q (2015) Synthesis of a Biotemplated Lithium Ion-Sieve Derived from Fungally Formed Birnessite. Advances in the Environmental Biogeochemistry of Manganese Oxides,

Song JF, Nghiem LD, Li XM, He TJESWR, Technology (2017) Lithium extraction from Chinese salt-lake brines: opportunities, challenges, and future outlook 3:593-597

Sw A, Yw A, Tao CA, Cl A, Yt BJCEJ Porous lithium ion sieves nanofibers: General synthesis strategy and highly selective recovery of lithium from brine water 379

Tomer VK, Malik R (2019) Hybridized Graphene for Chemical Sensing

Wen Z, Mou Y, Song Z, Xie L, Wang Y, Jing CJPiC (2017) Adsorption Materials for Lithium Ion from Brine Resources and Their Performances

Yang SS, Zhou ML, Wu JQ, Shen JN, Gao CJ Development and Adsorption Properties for a Novel Lithium Ion-Sieve. In: Materials Science Forum, 2016. pp 691-697

Zeng X, Mathews JA, Li JJES, Technology (2018) Urban Mining of E-Waste is Becoming More Cost-Effective Than Virgin Mining 52:4835–4841

Zhang, Zhang, Fusheng, Yongsheng, Zhongyu, Zheng, Xudong Dual-template docking oriented ionic imprinted bilayer mesoporous films with efficient recovery of neodymium and dysprosium

Zhang LY, Shui Y, Zhao LL, Zhu P, You YHJC (2019) Preparation of Ni-Doped Li2TiO3 Using an Inorganic Precipitation–Peptization Method 9:701

Zhao D, Xue-Min DU, Wang SQ, Guo YF, Deng TLJJoSS, Industry C (2017) Research on Extraction from Salt Lake Brine with High Mg/Li Ratio